



저작자표시-비영리-변경금지 2.0 대한민국

이용자는 아래의 조건을 따르는 경우에 한하여 자유롭게

- 이 저작물을 복제, 배포, 전송, 전시, 공연 및 방송할 수 있습니다.

다음과 같은 조건을 따라야 합니다:



저작자표시. 귀하는 원저작자를 표시하여야 합니다.



비영리. 귀하는 이 저작물을 영리 목적으로 이용할 수 없습니다.



변경금지. 귀하는 이 저작물을 개작, 변형 또는 가공할 수 없습니다.

- 귀하는, 이 저작물의 재이용이나 배포의 경우, 이 저작물에 적용된 이용허락조건을 명확하게 나타내어야 합니다.
- 저작권자로부터 별도의 허가를 받으면 이러한 조건들은 적용되지 않습니다.

저작권법에 따른 이용자의 권리는 위의 내용에 의하여 영향을 받지 않습니다.

이것은 [이용허락규약\(Legal Code\)](#)을 이해하기 쉽게 요약한 것입니다.

[Disclaimer](#)

이학석사학위논문

플루오린 치환기 없는 청색 이리듐  
발광체를 이용한 유기 발광 다이오드  
개발

**Blue Phosphorescent Iridium complexes  
with a Fluorine-free structure for  
Efficient Organic Light-Emitting Diodes**

2016년 8월

서울대학교 대학원 화학부

유기화학전공

신 화 용

**Blue Phosphorescent Iridium complexes with a  
Fluorine-free structure for Efficient Organic  
Light-Emitting Diodes**

by

**Hwa Yong Shin**

**Supervisor : Prof. Jong-In Hong**

**A Thesis for the Master Degree  
in Organic Chemistry**

**Department of Chemistry  
The Graduate School  
Seoul National University**

## Abstract

# Blue Phosphorescent Iridium complexes with a Fluorine-free structure for Efficient Organic Light-Emitting Diodes

Hwa Yong Shin

Major in Organic Chemistry

Department of Chemistry

The Graduate School

Seoul National University

Organic light-emitting diodes (OLEDs) attracts great attention because of its superior characteristics, such as for self-emitting, fast response time, high brightness, and applicability in flexible displays. In particular, phosphorescent OLEDs using iridium (III) complexes as emitters have been deeply studied for several decades. Its electrochemical stability, high quantum yield, and easy color tuning ability by controlling chelating ligands make iridium complexes prospective candidates as dopants.

Iridium(III)bis(4,6-(difluorophenyl)pyridinato-N,C<sup>2'</sup>)picolate (FIrpic), a sky-blue emitter, is widely used as a reference material for blue phosphorescent emitters. However, a deeper blue emission than FIrpic is needed to extend the color rendering range. For a deep blue emission, there

were many approaches to substituted electron-withdrawing groups, such as trifluoromethyl, trifluoromethylketone and perfluorobutanone, at 4-position of phenyl ring in FIrpic. However, according to previous studies, fluorine substitution appeared to degrade during sublimation and device operation.

In our study, we designed and synthesized blue phosphorescent iridium complexes without fluorine moiety. Three new compounds adapted 2-tert-butyl-5-(pyridin-2-yl)pyrimidine (b5ppmH) as a cyclometalated ligand as well as 2-(3-methyl-1H-1,2,4-triazol-5-yl)pyridine (mptz) and 2-(1H-tetrazol-5-yl)pyridine (ptz) as ancillary ligands to induce the blue emission. All compounds showed blue emission at 455-463nm with moderate quantum efficiencies. Photophysical, thermal, and electrochemical properties of the three new complexes were fully characterized. In addition, organic light emitting devices using complexes 1-3 were fabricated successfully and attained high external quantum efficiency of 11.5% with lower color coordinate y value than that of FIrpic.

**Keywords:** blue, fluorine-free, iridium complex, pyrimidine, OLED

**Student number:** 2014-22404

# Contents

<b>Abstract</b> .....	<b>1</b>
<b>Contents</b> .....	<b>3</b>
<b>A. Background</b>	
A.1. Introduction .....	4
A.2. Color Tuning Strategy .....	7
A.3. Blue Iridium Complexes .....	9
A.4. References .....	12
<b>B. Application</b>	
B.1. Blue phosphorescent iridium complexes with a fluorine-free structure for efficient organic light-emitting diodes	
B.1.1. Introduction .....	15
B.1.2. Result and Discussion .....	18
B.1.3. Experimental Sections .....	34
B.1.4. References .....	39
<b>국문초록</b> .....	<b>40</b>
<b>감사의 글</b> .....	<b>42</b>

# A. Background

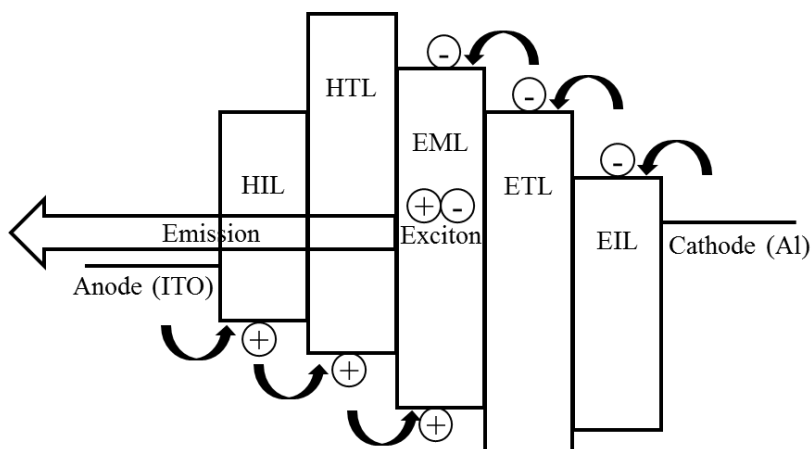
## A.1. Introduction

The photophysical properties of octahedral metal complexes have been studied thoroughly for several decades. Ruthenium and Osmium complexes were used in diverse photonic applications like photocatalysis and photoelectrochemistry.<sup>1</sup> The preference for  $d^6$  complexes are due to their long-lived excited states, high quantum efficiencies, and high photosensitization capacity for electron or energy transfer. Heavy metals in  $d^6$  complexes induce strong spin-orbit coupling which lead to an efficient intersystem crossing from singlet to triplet state. By mixing singlet and triplet excited state via strong spin orbit coupling, the spin-forbidden nature of radiative triplet excited state is removed.<sup>2</sup> This enhances the phosphorescent efficiency.

The triplet states of iridium(III) complexes are advantageous over those of other transition metal complexes in that their electronic transitions and charge-transfer characteristics are tunable over wide ranges. The electronic transition responsible for luminescence is assigned to a mixture of metal to ligand charge transfer ( $^3MLCT$ ) and ligand centered ( $^3LC$ ) transition characteristics.<sup>3</sup> Highly emissive iridium(III) complexes are composed of two cyclometalated ligands (abbreviate as  $C^N$ ) and a single monoanionic, bidentate ancillary ligand (LX). Due to MLCT and LC components in the lowest triplet excited state ( $T_1$ ) of iridium(III) complexes, emission colors are

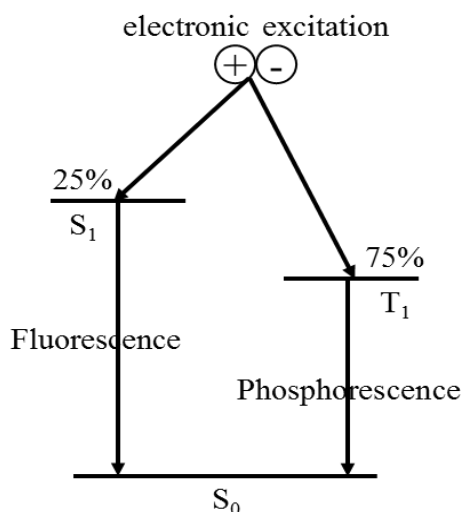
strongly dependent on cyclometalating ligands. A variety of C<sup>^</sup>N ligands allows emission wavelength tuning across the entire visible spectrum. These favorable properties made iridium(III) complexes leading candidates in electroluminescence.<sup>2b</sup>

Iridium (III) complexes can serve as efficient phosphors in organic light emitting diodes (OLEDs). In OLEDs, holes and electrons are injected from anode and cathode, respectively, on the other side of the devices. They then pass through several organic layers and interfaces. Finally, they recombine to form excitons, or radiative excited states in the emitting layer. Excitons are relaxed to the ground state and the light with certain wavelength is emitted. Electrically generated excitons can be either singlet or triplet in 1 to 3 ratio.<sup>4</sup> Fluorescent materials can only use singlet excitons in order to be radiatively relaxed. This implies that fluorescent OLED inherently limited the internal



**Figure 1.** Basic structure and mechanism of OLEDs.



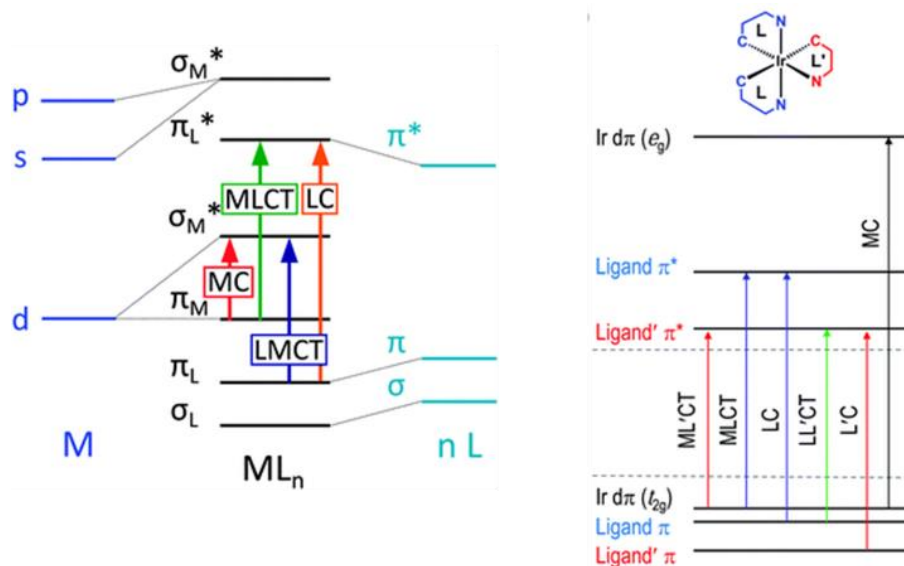


**Figure 2.** Light emitting mechanism of emitters.

quantum efficiency to 25%. On the other hand, when iridium complexes are emitters, a heavy metal effect induces strong spin-orbit coupling and singlet-triplet mixing. Therefore, the internal quantum efficiency of phosphorescent OLED can reach a theoretical level of unity. The internal quantum efficiency reached nearly 100% under the assumption that coefficients of charge balance and excitation possibility were unity.<sup>5</sup> OLEDs have been prepared with  $(C^{\wedge}N)_2Ir(LX)$  phosphorescent dopants exhibiting efficient blue, green, yellow, or red emissions. The external quantum efficiency of phosphorescent OLEDs reached up to 30% with considerable effort.<sup>6</sup>

## A.2. Color Tuning Strategy

The color tuning ability of iridium (III) complexes is the most intriguing point among its strengths, such as electrochemical stability, high quantum efficiency and short lifetime. In molecular orbitals of common metal complexes, the frontier transition is predominantly determined by metal centered transition (MC) characteristics.<sup>7</sup> As a result, variations in ligands have little effect on emission wavelength unless the center metal is replaced. On the contrary, the  $d\pi$ -orbital of iridium complexes is positioned at high energy levels. Iridium complexes have ligand characteristics in frontier transition, such as metal to ligand transition (MLCT), ligand centered transition (LC), and ligand to ligand transition (LLCT). As a result, by tuning the ligand framework, the energy gap can be controlled in a predictable way.<sup>8</sup>



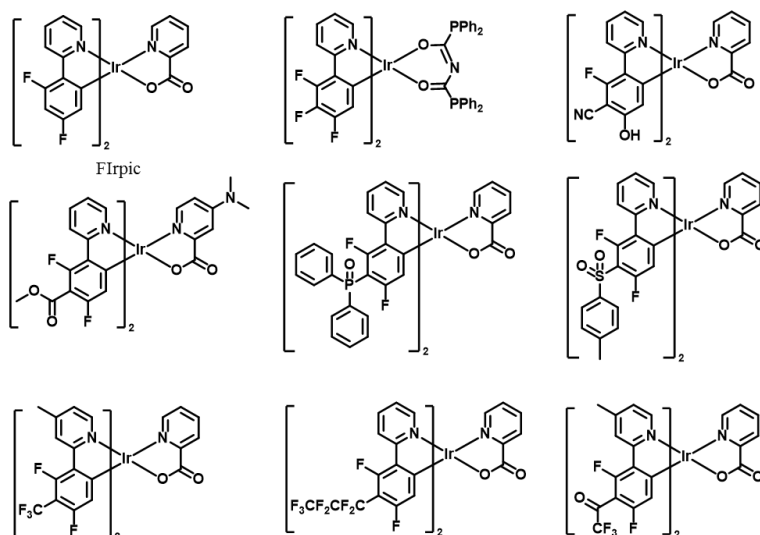
**Figure 3.** Molecular orbitals and transition characteristics of common metal complexes (left) and iridium complexes (right).

$\text{Ir}(\text{ppy})_3$ , Tris[2-phenylpyridinato-C2,N]iridium(III), which is composed of three phenylpyridine cyclometalated ligands, is the starting point for the color tuning strategy of iridium(III) complexes. In this complex, the highest occupied molecular orbital (HOMO) is predominantly distributed on the iridium d-orbital and phenyl ring of the cyclometalated ligand. The lowest unoccupied molecular orbital (LUMO) mainly resides on the pyridyl  $\pi^*$ -orbitals of cyclometalated ligands. By applying the electron withdrawing or donating groups to cyclometalated ligands, the energy levels are stabilized or destabilized, respectively. Using this strategy, researchers can change the emission wavelength of iridium complexes from red to blue.

### A.3. Blue Iridium Complexes

Red, green, and blue emitters are needed for a full color display. Efficient red and green iridium complexes have been successively investigated for PHOLEDs.<sup>9</sup> However, the development of efficient blue iridium complexes is still challenge. The Forrest and Thompson group was a pioneer of using FIrpic, bis(2-(4',6'-difluoro)phenylpyridinato- N,C2')<sub>2</sub>iridium(III) picolinate as a sky-blue emitter.<sup>10</sup> FIrpic employs phenylpyridine cyclometalated ligands substituted with fluorines, or electron-withdrawing groups, to stabilize the HOMO energy level. By enlarging the energy gap, FIrpic exhibits blue-shifted emission at 470 and 492nm in contrast to Ir(ppy)<sub>3</sub>, tris(2-phenylpyridinato)iridium which emits at 507nm.<sup>11</sup> FIrpic is widely investigated as a reference material for blue phosphorescent OLEDs.<sup>12</sup> However, true-blue emitters are in demand for a high color reproduction range. Further functionalization has been conducted for several years in order to produce deep blue emitting materials.

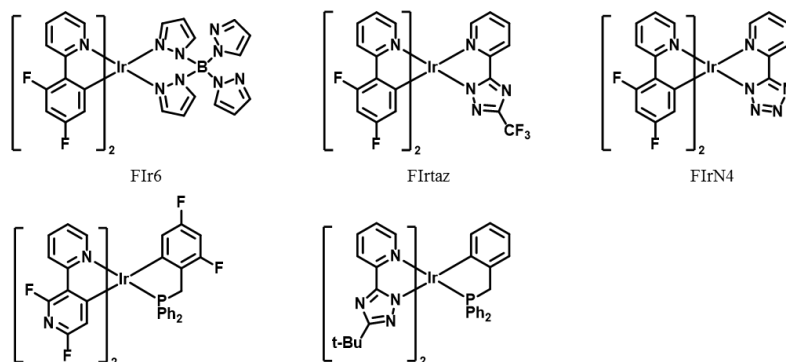
A series of iridium complexes which add electron withdrawing groups at the 5'-position of phenyl ring in FIrpic were synthesized to stabilize the HOMO level of iridium complexes. For example, fluoro,<sup>13</sup> cyano,<sup>14</sup> ester,<sup>15</sup> phosphoryl, sulfonyl,<sup>16</sup> trifluoromethyl,<sup>17</sup> and other fluorinated alkyls<sup>18</sup> were used to induce deeper HOMO levels. This method is the most popular way achieve deep blue emission. However, this strategy has several problems. Overly strong electron withdrawing groups, such as perfluoro carbonyl



**Figure 4.** Blue phosphorescent iridium complexes with electron withdrawing substitution at 5'-position of phenyl ring in cyclometalated ligands.

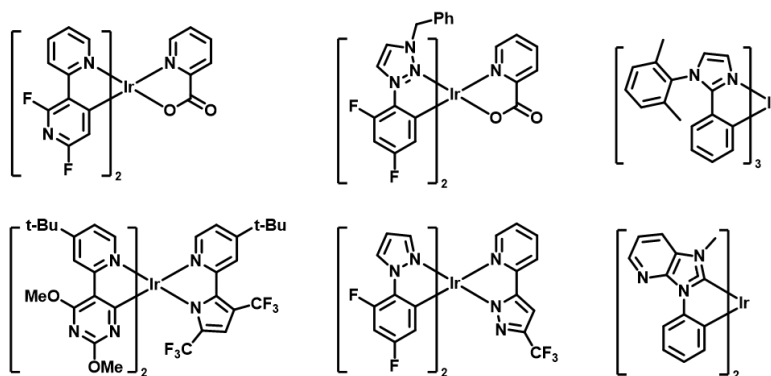
groups<sup>18b</sup> can stabilize not only HOMO levels but also LUMO levels. In addition, fluorine substitution is vulnerable to degradation during sublimation and device operation.<sup>19</sup>

Another way is to apply electron deficient ancillary ligands. Ancillary ligands can participate in frontier transition characteristics by affecting iridium  $d\pi$  orbitals. For example, FIr6,<sup>20</sup> FIrtaZ and FIrN4<sup>21</sup> which has tetra-pyrazole



**Figure 5.** Blue phosphorescent iridium complexes with electron-deficient ancillary ligands.

borate, trifluoromethyl pyridyl triazolate and 2-pyridyl tetrazolate act as ancillary ligands. Benzyldiphenylphosphines were also used to induce blue



**Figure 6.** Blue phosphorescent iridium complexes having heteroaromatic rings.

shift without elongation of conjugated system.<sup>22</sup>

Another method is to replace phenyl or pyridyl rings with heteroaromatic rings to increase the  $\pi$ - $\pi^*$  energy gap. Recently, studies about blue phosphorescent iridium complexes with bipyridine ligands have become popular.<sup>23</sup> Triazole,<sup>22b, 24</sup> imidazole,<sup>25</sup> pyrimidine<sup>26</sup> and pyrazole<sup>27</sup> are also utilized as alternatives. An iridium complex composed of phenylpyridylimidazole has also been reported.<sup>28</sup> In this paper, the Forrest group achieved very high brightness and efficiency with deep blue emission.

However, additional studies are needed to develop deep-blue emitters with good color purity, long term stability, and high quantum efficiency.

## A.4. References

1. (a) Chin, K. F.; Cheung, K. K.; Yip, H. K.; Mak, T. C. W.; Che, C. M., *J Chem Soc Dalton* **1995**, 657-663; (b) Kalyanasundaram, K., *Coord. Chem. Rev.* **1982**, *46*, 159-244.
2. (a) Baldo, M. A.; Lamansky, S.; Burrows, P. E.; Thompson, M. E.; Forrest, S. R., *Appl. Phys. Lett.* **1999**, *75*, 4-6; (b) Baldo, M. A.; O'Brien, D. F.; You, Y.; Shoustikov, A.; Sibley, S.; Thompson, M. E.; Forrest, S. R., *Nature* **1998**, *395*, 151-154.
3. Wilde, A. P.; King, K. A.; Watts, R. J., *J. Phys. Chem.* **1991**, *95*, 629-634.
4. Baldo, M. A.; O'Brien, D. F.; Thompson, M. E.; Forrest, S. R., *Phys Rev B* **1999**, *60*, 14422-14428.
5. Adachi, C.; Baldo, M. A.; Thompson, M. E.; Forrest, S. R., *J. Appl. Phys.* **2001**, *90*, 5048-5051.
6. (a) Kim, K. H.; Lee, S.; Moon, C. K.; Kim, S. Y.; Park, Y. S.; Lee, J. H.; Lee, J. W.; Huh, J.; You, Y.; Kim, J. J., *Nat. Commun.* **2014**, *5*; (b) Kim, S. Y.; Jeong, W. I.; Mayr, C.; Park, Y. S.; Kim, K. H.; Lee, J. H.; Moon, C. K.; Brutting, W.; Kim, J. J., *Adv. Funct. Mater.* **2013**, *23*, 3896-3900; (c) Udagawa, K.; Sasabe, H.; Cai, C.; Kido, J., *Adv. Mater.* **2014**, *26*, 5062-5066.
7. Heine, J.; Muller-Buschbaum, K., *Chem. Soc. Rev.* **2013**, *42*, 9232-9242.
8. You, Y.; Nam, W., *Chem. Soc. Rev.* **2012**, *41*, 7061-7084.
9. (a) Liang, B.; Jiang, C. Y.; Chen, Z.; Zhang, X. J.; Shi, H. H.; Cao, Y., *J. Mater. Chem.* **2006**, *16*, 1281-1286; (b) Lu, K. Y.; Chou, H. H.; Hsieh, C. H.; Yang, Y. H. O.; Tsai, H. R.; Tsai, H. Y.; Hsu, L. C.; Chen, C. Y.; Chen, I. C.; Cheng, C. H., *Adv. Mater.* **2011**, *23*, 4933-4937; (c) Xiao, L. X.; Chen, Z. J.; Qu, B.; Luo, J. X.; Kong, S.; Gong, Q. H.; Kido, J. J., *Adv. Mater.* **2011**, *23*, 926-952.
10. (a) Adachi, C.; Kwong, R. C.; Djurovich, P.; Adamovich, V.; Baldo, M. A.; Thompson, M. E.; Forrest, S. R., *Appl. Phys. Lett.* **2001**, *79*, 2082-2084; (b) Kawamura, Y.; Yanagida, S.; Forrest, S. R., *J. Appl. Phys.* **2002**, *92*, 87-93.
11. Lamansky, S.; Djurovich, P.; Murphy, D.; Abdel-Razzaq, F.; Kwong, R.; Tsyba, I.; Bortz, M.; Mui, B.; Bau, R.; Thompson, M. E., *Inorg. Chem.* **2001**, *40*, 1704-1711.
12. Sasabe, H.; Minamoto, K.; Pu, Y. J.; Hirasawa, M.; Kido, J., *Org. Electron.* **2012**, *13*, 2615-2619.

13. Wang, C. C.; Jing, Y. M.; Li, T. Y.; Xu, Q. L.; Zhang, S.; Li, W. N.; Zheng, Y. X.; Zuo, J. L.; You, X. Z.; Wang, X. Q., *Eur. J. Inorg. Chem.* **2013**, *2013*, 5683-5693.
14. Kozhevnikov, V. N.; Dahms, K.; Bryce, M. R., *J. Org. Chem.* **2011**, *76*, 5143-5148.
15. Marin-Suarez, M.; Curchod, B. F. E.; Tavernelli, I.; Rothlisberger, U.; Scopelliti, R.; Jung, I.; Di Censo, D.; Gratzel, M.; Fernandez-Sanchez, J. F.; Fernandez-Gutierrez, A.; Nazeeruddin, M. K.; Baranoff, E., *Chem. Mater.* **2012**, *24*, 2330-2338.
16. Fan, C.; Li, Y. H.; Yang, C. L.; Wu, H. B.; Qin, J. G.; Cao, Y., *Chem. Mater.* **2012**, *24*, 4581-4587.
17. (a) Park, H. J.; Kim, J. N.; Yoo, H. J.; Wee, K. R.; Kang, S. O.; Cho, D. W.; Yoon, U. C., *J. Org. Chem.* **2013**, *78*, 8054-8064; (b) Yun, S. J.; Seo, H. J.; Song, M.; Jin, S. H.; Kang, S. K.; Kim, Y. I., *J. Organomet. Chem.* **2013**, *724*, 244-250.
18. (a) Kim, J. B.; Han, S. H.; Yang, K.; Kwon, S. K.; Kim, J. J.; Kim, Y. H., *Chem. Commun.* **2015**, *51*, 58-61; (b) Lee, S.; Kim, S. O.; Shin, H.; Yun, H. J.; Yang, K.; Kwon, S. K.; Kim, J. J.; Kim, Y. H., *J. Am. Chem. Soc.* **2013**, *135*, 14321-14328.
19. Sivasubramaniam, V.; Brodkorb, F.; Hanning, S.; Loebel, H. P.; van Elsbergen, V.; Boerner, H.; Scherf, U.; Kreyenschmidt, M., *J. Fluorine Chem.* **2009**, *130*, 640-649.
20. Li, J.; Djurovich, P. I.; Alleyne, B. D.; Tsyba, I.; Ho, N. N.; Bau, R.; Thompson, M. E., *Polyhedron* **2004**, *23*, 419-428.
21. Yeh, S. J.; Wu, M. F.; Chen, C. T.; Song, Y. H.; Chi, Y.; Ho, M. H.; Hsu, S. F.; Chen, C. H., *Adv. Mater.* **2005**, *17*, 285-289.
22. (a) Hung, J. Y.; Chi, Y.; Pai, I. H.; Yu, Y. C.; Lee, G. H.; Chou, P. T.; Wong, K. T.; Chen, C. C.; Wu, C. C., *Dalton Trans.* **2009**, 6472-6475; (b) Chang, C. H.; Ho, C. L.; Chang, Y. S.; Lien, I. C.; Lin, C. H.; Yang, Y. W.; Liao, J. L.; Chi, Y., *J. Mater. Chem. C* **2013**, *1*, 2639-2647.
23. (a) Bejoomohandas, K. S.; Kumar, A.; Varughese, S.; Varathan, E.; Subramanian, V.; Reddy, M. L. P., *J. Mater. Chem. C* **2015**, *3*, 7405-7420; (b) Kang, Y.; Chang, Y. L.; Lu, J. S.; Ko, S. B.; Rao, Y. L.; Varlan, M.; Lu, Z. H.; Wang, S. N., *J. Mater. Chem. C* **2013**, *1*, 441-450; (c) Lee, J.; Oh, H.; Kim, J.; Park, K. M.; Yook, K. S.; Lee, J. Y.; Kang, Y., *J. Mater. Chem. C* **2014**, *2*, 6040-6047.
24. (a) Fernandez-Hernandez, J. M.; Beltran, J. I.; Lemaur, V.; Galvez-Lopez, M. D.; Chien, C. H.; Polo, F.; Orselli, E.; Frohlich, R.; Cornil, J.; De Cola, L., *Inorg.*



- Chem.* **2013**, *52*, 1812-1824; (b) Li, H.; Yin, Y. M.; Cao, H. T.; Sun, H. Z.; Wang, L.; Shan, G. G.; Zhu, D. X.; Su, Z. M.; Xie, W. F., *J. Organomet. Chem.* **2014**, *753*, 55-62.
25. (a) Klubek, K. P.; Dong, S. C.; Liao, L. S.; Tang, C. W.; Rothberg, L. J., *Org. Electron.* **2014**, *15*, 3127-3136; (b) Zhuang, J. Y.; Li, W. F.; Wu, W. C.; Song, M. S.; Su, W. M.; Zhou, M.; Cui, Z., *New J. Chem.* **2015**, *39*, 246-253.
26. (a) Chang, C. H.; Wu, Z. J.; Chiu, C. H.; Liang, Y. H.; Tsai, Y. S.; Liao, J. L.; Chi, Y.; Hsieh, H. Y.; Kuo, T. Y.; Lee, G. H.; Pan, H. A.; Chou, P. T.; Lin, J. S.; Tseng, M. R., *Acs Appl Mater Inter* **2013**, *5*, 7341-7351; (b) Duan, T.; Chang, T. K.; Chi, Y.; Wang, J. Y.; Chen, Z. N.; Hung, W. Y.; Chen, C. H.; Lee, G. H., *Dalton Trans.* **2015**, *44*, 14613-14624.
27. Yang, C. H.; Li, S. W.; Chi, Y.; Cheng, Y. M.; Yeh, Y. S.; Chou, P. T.; Lee, G. H.; Wang, C. H.; Shu, C. F., *Inorg. Chem.* **2005**, *44*, 7770-7780.
28. Lee, J.; Chen, H. F.; Batagoda, T.; Coburn, C.; Djurovich, P. I.; Thompson, M. E.; Forrest, S. R., *Nat. Mater.* **2016**, *15*, 92-99.

## **B. Application**

### **B.1. Blue Phosphorescent Iridium complexes with a Fluorine-free structure for Efficient Organic Light-Emitting Diodes**

#### **B.1.1. Introduction**

For the last two decades, organic light emitting diodes (OLEDs) have received attention for the next generation of displays. Iridium based complexes are studied due to their outstanding features such as thermal and electrochemical stability, short excited lifetime, high quantum efficiency, and facile color tuning ability spanning all visible regions.<sup>1</sup> The three elementary colors, red, green and blue are needed to realized natural light. Red and green emitting phosphors have been developed with good color purity and high quantum efficiency.<sup>2</sup> However, blue emitters that attain good color purity and high quantum yield simultaneously are still a challenge. The reason for the late advance in blue emitters is due to higher lying lowest excited triplet state ( $T_1$ ).<sup>3</sup>

The emission wavelength can be tuned by carefully designing ligands that bound to an iridium metal center. There are fundamental strategies to induce blue emission wavelength; stabilizing the highest occupied molecular orbital (HOMO) energy level by utilizing electron withdrawing groups and destabilizing the lowest unoccupied molecular level (LUMO) with electron

donating groups. HOMO is well known to reside mainly on phenyl ring of cyclometalated ligands while LUMO is predominantly localized at the pyridine ring of cyclometalated ligands. Therefore, substituting electron withdrawing (or donating groups) to phenyl (or pyridine) rings lead to high energy gaps. These strategies cause gap enlargement between HOMO and LUMO; that is, a hypsochromic shift. Representatively, FIrpic uses fluorines on the phenyl rings of main ligands to stabilize the HOMO level and emits sky-blue light at 472nm. The other strategy is by replacing the phenyl ring with other heteroaromatic rings which have larger  $\pi$ - $\pi^*$  energy gaps. Blue shift was achieved by using pyridines,<sup>4</sup> pyrimidines,<sup>5</sup> and triazoles.<sup>6</sup> Stabilizing HOMO with electron deficient groups like fluorine and its derivatives was commonly studied.

However, fluorine substitution has lethal problems. C-F cleavage arises during sublimation and device operation,<sup>7</sup> so fluorine-free blue emitters are needed to improve the lifetime of blue phosphorescent OLEDs.

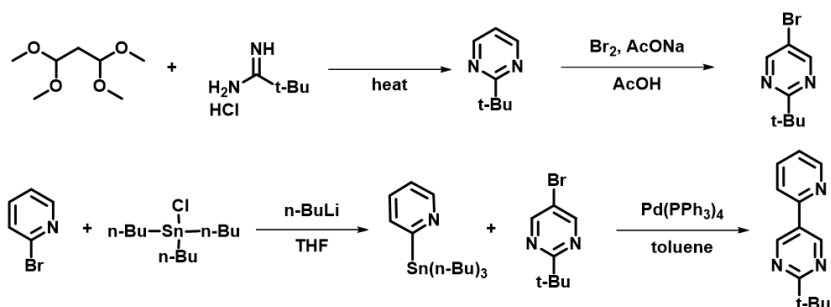
In this thesis, we discuss fluorine-free blue phosphorescent iridium complexes with pyridylpyrimidine as main ligands. The pyridylpyrimidine ligand has larger  $\pi$ - $\pi^*$  energy gap than the phenyl pyridine ligand which induces blue shift of emission. We synthesized complex **1** with picolate ancillary ligand (pic) to compare the effect of the main ligand to emission wavelength with the representative blue emitter, iridium(III)bis(4,6-(difluorophenyl)pyridinato-N,C2')picolate (FIrpic). Additionally, complexes with 2-(3-methyl-1H-1,2,4-triazol-5-yl)pyridine (mptz) (**2**) or 2-(1H-tetrazol-5-

yl)pyridine (ptz) (**3**) as ancillary ligands were synthesized to induce further blue shift of the emission. They showed good thermal properties, quantum efficiency, and low color coordinate  $\gamma$  compared to FIrpic. The OLED device based on iridium complex **3** with a fluorine-free structure exhibited a maximum external quantum efficiency of 11.5% and a good color coordinate (0.17, 0.26). The associated details and results are presented in proceeding sections.

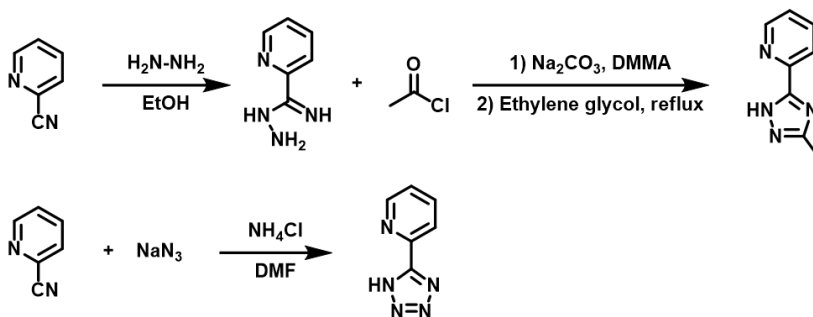
## B.1.2. Result and Discussion

### Synthesis

#### Main ligand

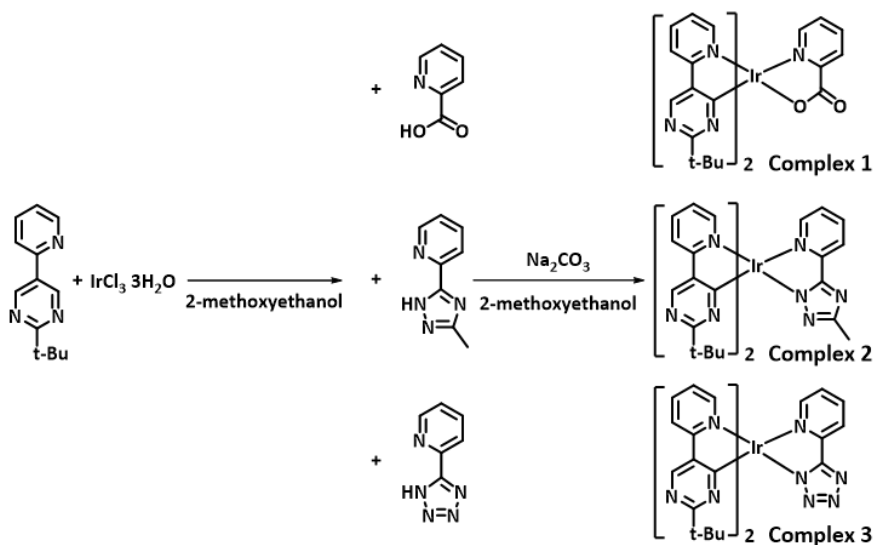


#### Ancillary ligand



**Scheme 1.** Synthetic procedures of main and ancillary ligands.

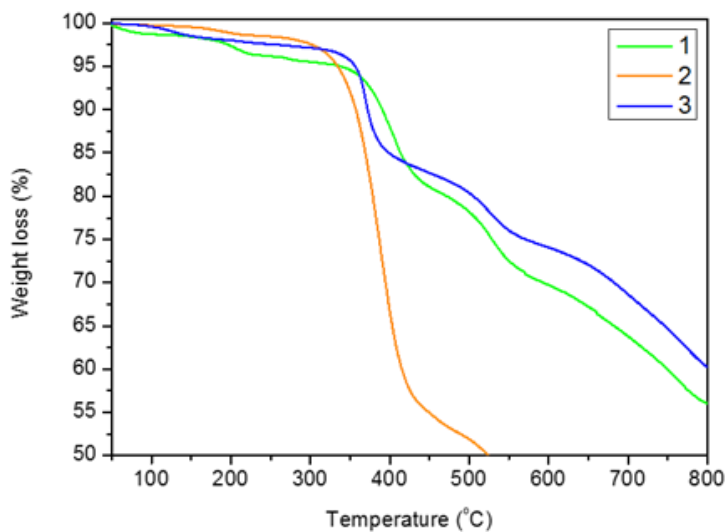
The synthetic procedures of complexes **1**, **2**, and **3** are shown in Schemes 1 and 2. 2-Tert-butylpyrimidine was prepared and bromination was conducted. Then, 2-tert-butyl-5-(pyridin-2-yl)pyrimidine (b5ppmH) was synthesized through an Ullmann coupling reaction with 2-tributylstannylpyridine. Dichloro-bridged iridium dimers were obtained by heating a mixture of b5ppmH and IrCl<sub>3</sub>·nH<sub>2</sub>O at reflux in 2-methoxyethanol. Complexes **1-3** were prepared by adding ancillary ligands to iridium dimers in the presence of Na<sub>2</sub>CO<sub>3</sub>. All synthesized complexes were characterized by



**Scheme 2.** Synthetic procedures of complexes 1-3.

nuclear magnetic resonance (NMR) spectroscopy and high resolution mass spectra (HRMS). The Experimental section details this process.

### Thermal Stability

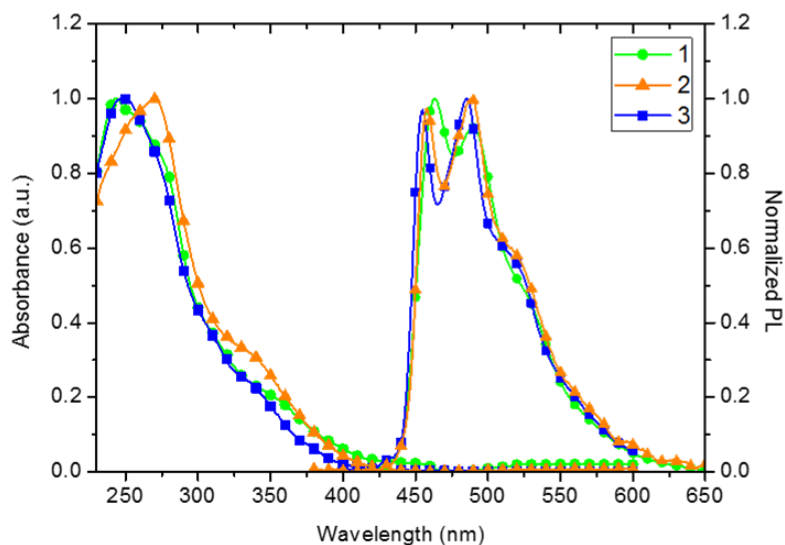


**Figure 1.** TGA curves of complexes 1-3.

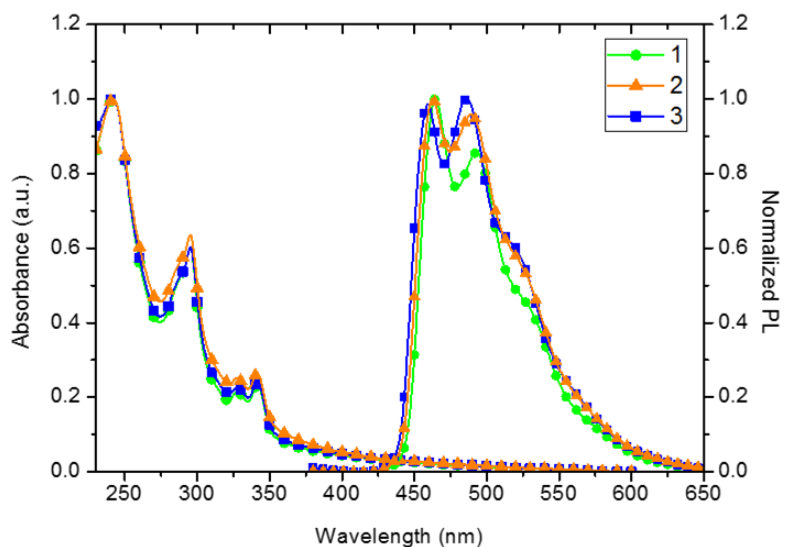
To investigate the thermal stabilities of three iridium complexes, thermal gravimetric analysis (TGA) was carried out. Generally, materials with decomposition temperatures above 300 °C are suitable to vacuum deposition without degradation during OLED manufacturing.<sup>8</sup> The temperatures at which 5 % weight loss occur are determined to be decomposition temperatures of the compounds. As shown in Figure 1, complexes **1**, **2**, and **3** showed decomposition temperatures at 339, 334, and 356 °C, respectively. Such high thermal stability are attributed to the fluorine-free structure, which enables complexes **1**, **2**, and **3** to be deposited by thermal evaporation. In addition, these materials would guarantee good morphological stability and stable device operation.

### **Photophysical Properties**

The absorption and phosphorescent emission spectra of the three iridium complexes in dichloromethane at room temperature are shown in Figure 2 and photophysical data are summarized in Table 1. In absorption spectra, complexes **1** and **3** showed similar spectral pattern except for complex **2** exhibited red shifted absorption. The intense absorption at 230-270 nm of complexes **1**, **2**, and **3** is ascribed from the allowed ligand centered (<sup>1</sup>LC) transition of cyclometalated ligands. The absorption bands at around 350 nm are attributed to the allowed metal to ligand charge



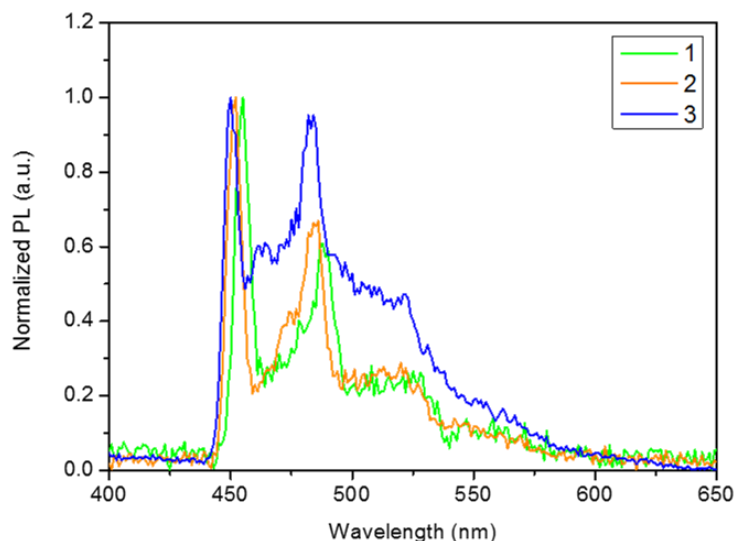
**Figure 2.** Absorption and photoluminescent (PL) spectra of complexes **1-3** at room temperature in  $\text{CH}_2\text{Cl}_2$ .



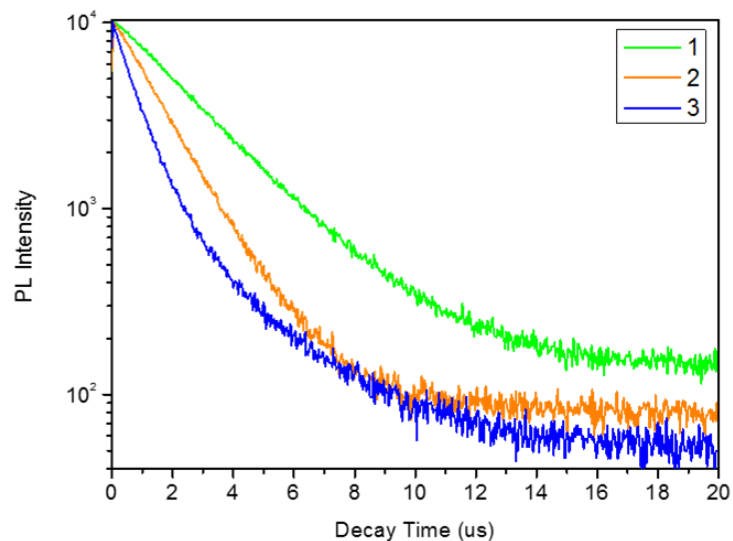
**Figure 3.** Absorption and PL spectra of complexes **1-3** at room temperature in 10 wt% doped mCP film.

transfer ( $^1\text{MLCT}$ ) transition. The weak absorption region over  $\sim 380$  nm is assigned to the mixture of forbidden ligand centered transition and metal to ligand charge transfer transition ( $^3\text{LC}$  and  $^3\text{MLCT}$ ). In emission spectra, all complexes exhibited significant blue shifted emission





**Figure 4.** PL spectrum of complexes **1-3** at 77K in 2-MeTHF.



**Figure 5.** Transient PL of complexes **1-3** at room temperature in toluene.

compared to the sky-blue emitter, iridium(III)bis(4,6-(difluorophenyl)pyridinato- $N,C^{2'}$ )picolinate (FIrpic). When excited by 340nm radiation, three complexes showed intense blue emissions with the first peak maxima at 463, 458, and 455nm for complexes **1**, **2**, and **3**, respectively. Without fluorine moiety, all compounds achieved blue

emission. The replacement of phenyl groups with pyrimidine rings lead to larger  $\pi$ - $\pi^*$  ligand transition energy and contributed to the blue shift of emission wavelength. By replacing picolinate ligand with mptz and ptz ligands, the emission wavelength shows a hypsochromic shift about 5-8 nm. The emission is strongly dependent on the nature of ancillary ligands, so complex **3** exhibited the shortest wavelength emission. Pyridyltetrazolate of complex **3** has stronger electron withdrawing ability than pyridyltriazolate of complex **2**. This further stabilizes the HOMO energy level of complex **3** and leads to the largest energy gap among three complexes. The compounds exhibited well-structured emission profiles at room temperature. According to previous studies,<sup>9</sup> the lowest excited triplet states ( $T_1$ ) of the complexes which have dominant  $^3LC$  characteristics mixed with  $^3MLCT$  contribution showed sharp and well-structured emission features. With dominant  $^3MLCT$  characteristic in the lowest triplet state, the emission exhibits broad and structureless features. The phosphorescence of all three compounds were predominantly from  $\pi$ - $\pi^*$  characteristics with minor contribution from  $MLCT$  characteristics. The low temperature PL at 77K also supported emissions mainly originating from ligand centered transitions (Figure 4). The photoluminescent spectra at 77K displayed highly resolved vibrational features with slightly blue shifted emission wavelength. Triplet energies ( $E_T$ ) of three complexes were deduced to 2.73, 2.74, and 2.76 eV for complexes **1**, **2**, and **3**, respectively. In the film state, all compounds

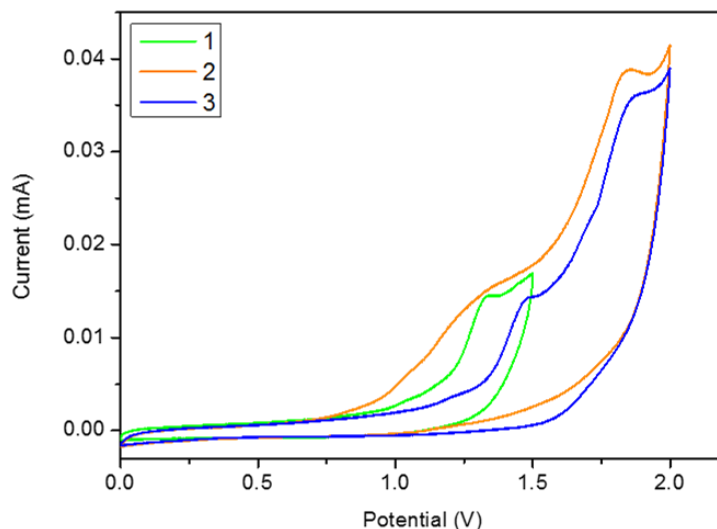
showed bathochromic shift at about 2-4nm. In the solid state, aggregations and intermolecular interactions occur and induce red shift of emission wavelength (Figure 3). The quantum yields were also calculated using FIrpc as a reference ( $\Phi = 0.60$ ).  $\Phi$  is 0.65 for complex **1**, 0.41 for complex **2**, and 0.43 for complex **3**. Three compounds had high quantum efficiencies suitable for OLED emitters. We also investigated the characteristics of decay rates through time-resolved phosphorescence lifetime measurements. The observed lifetimes were 2.53, 1.47, and 0.768  $\mu$ s for complexes **1**, **2**, and **3**. The microsecond order lifetimes imply that the emissions were derived from the phosphorescence of iridium complexes (Figure 5).

**Table 1.** Photophysical properties of complexes **1-3**.

Complex	$\lambda_{\text{abs}}^{\text{a}}$ (nm)	$\lambda_{\text{em, RT}}^{\text{a}}$ solution <sup>a</sup> / film <sup>b</sup> (nm)	$\lambda_{\text{em, 77K}}^{\text{c}}$ (nm)	$\Phi^{\text{d}}$	$\tau_{\text{obs}}^{\text{e}}$ ( $\mu$ s)	$k_{\text{r}}^{\text{f}}$ ( $10^5 \text{ s}^{-1}$ )	$k_{\text{nr}}^{\text{f}}$ ( $10^5 \text{ s}^{-1}$ )	$E_{\text{T}}$ (eV)	$E_{\text{gap}}$ (eV)	HOMO / LUMO <sup>g</sup> (eV)
<b>1</b>	244, 354	463, 490 / 465, 493	455	0.54	2.53	2.13	1.82	2.73	2.95	-5.51 / - 2.56
<b>2</b>	269, 338	458, 489 / 463, 490	452	0.43	1.49	2.75	3.96	2.74	3.06	-5.56 / - 2.59
<b>3</b>	249, 337	455, 485 / 459, 486	450	0.46	0.768	5.99	7.03	2.76	3.17	-5.91 / - 2.74

<sup>a</sup> Measured in DCM solution at  $[M] = 1.0 \times 10^{-5}$  M. <sup>b</sup> Doped into mCP at 10wt%. <sup>c</sup> In frozen 2-Methyl tetrahydrofuran matrix at  $[M] = 1.0 \times 10^{-5}$  M. <sup>d</sup> Phosphorescence quantum efficiency was measured in DCM relative to FIrpc ( $\Phi = 0.60$ ). <sup>e</sup> Measured in toluene solution at  $[M] = 1.0 \times 10^{-4}$ . <sup>f</sup> Calculated by equations;  $k_{\text{r}} = \Phi/\tau_{\text{obs}}$ ,  $k_{\text{nr}} = (1-\Phi)/\tau_{\text{obs}}$ . <sup>g</sup> HOMO was estimated from their corresponding oxidation potential obtained from CV experiment. LUMO = HOMO +  $E_{\text{gap}}$ .

## Electrochemical Properties



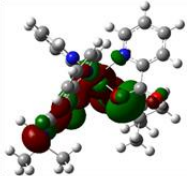

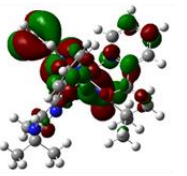
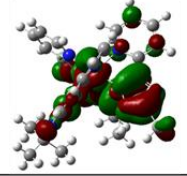
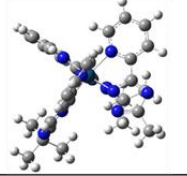
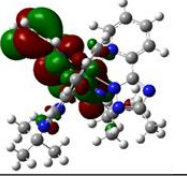
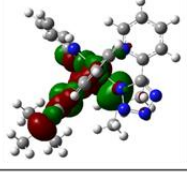
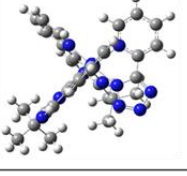
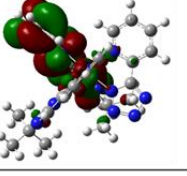
**Figure 6.** Cyclic voltammetry of complexes **1-3** at room temperature.

To investigate the electrochemical properties of complexes **1**, **2**, and **3**, cyclic voltammetry measurement was conducted. As shown in Figure 6, all compounds exhibited irreversible oxidation in dichloromethane at room temperature. Oxidation potentials ( $E_{ox}$ ) of complexes **1**, **2**, and **3** were 0.98, 1.12, and 1.38 eV, respectively. Using ferrocene as a reference, the HOMO levels of compounds were deduced to be -5.51, -5.56, and -5.91 V for complexes **1**, **2**, and **3**, respectively.  $E_{gap}$  was obtained from the absorption edges to be 2.95, 3.06, and 3.17 eV for complexes **1**, **2**, and **3**. The LUMO levels were estimated via equation  $E_{LUMO} = (E_{HOMO} + E_{gap})$  eV. Compounds using electron-deficient ancillary ligands, complexes **2** and **3**, appeared with more stabilized HOMO levels compared to the pic. As the electron withdrawing ability of ancillary ligands increases, the energy level of HOMO becomes more stabilized.

The HOMO stabilization is stronger than LUMO stabilization and leads to an increased energy gap in complexes **2** and **3**.

### **Theoretical Calculation**

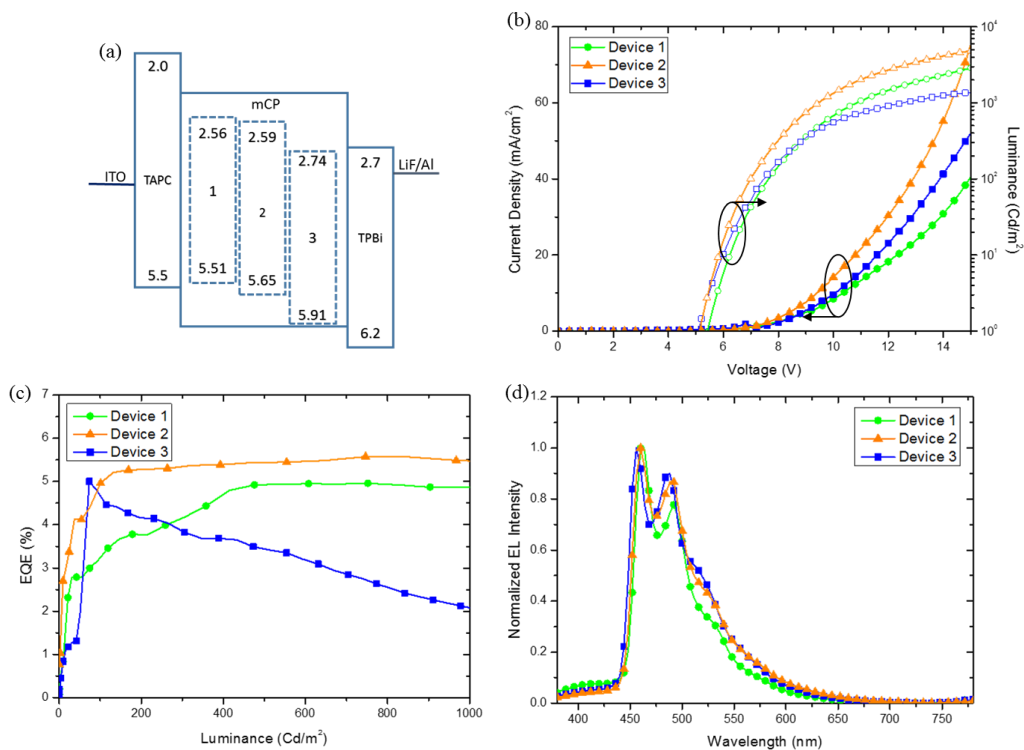
To evaluate the energy levels and orbital electron density distributions of HOMO and LUMO, density functional theory calculations were employed. The geometries of three compounds were under optimized positions and showed distorted octahedral structures around the iridium metal atoms. Significant frontier molecular orbitals for iridium complexes are presented in Figure 7. The HOMO of complexes **1** and **3** is mainly distributed on the iridium d-orbital and pyrimidine  $\pi$  orbital of cyclometalated ligands. In complex **2**, HOMO mainly resides on the iridium d-orbital and pyrimidine  $\pi$  orbital with small contribution from ancillary ligand. The contribution from mptz ancillary ligand causes higher HOMO level of complex **2** than that of complex **1**. The LUMO of three complexes exists at almost the same position,  $\pi^*$ orbital of pyridine and pyrimidine in cyclometalated ligand, except for contribution from picolinic acid in complex **1**. Hence, the transition is mostly governed by LC characteristics, coinciding with emission profile discussed previously.

HOMO	Structure	LUMO
		
5.67eV	Complex 1	2.17eV
		
5.56eV	Complex 2	2.11eV
		
5.77eV	Complex 3	2.29eV

**Figure 7.** Calculated frontier molecular orbitals of complexes **1-3**.

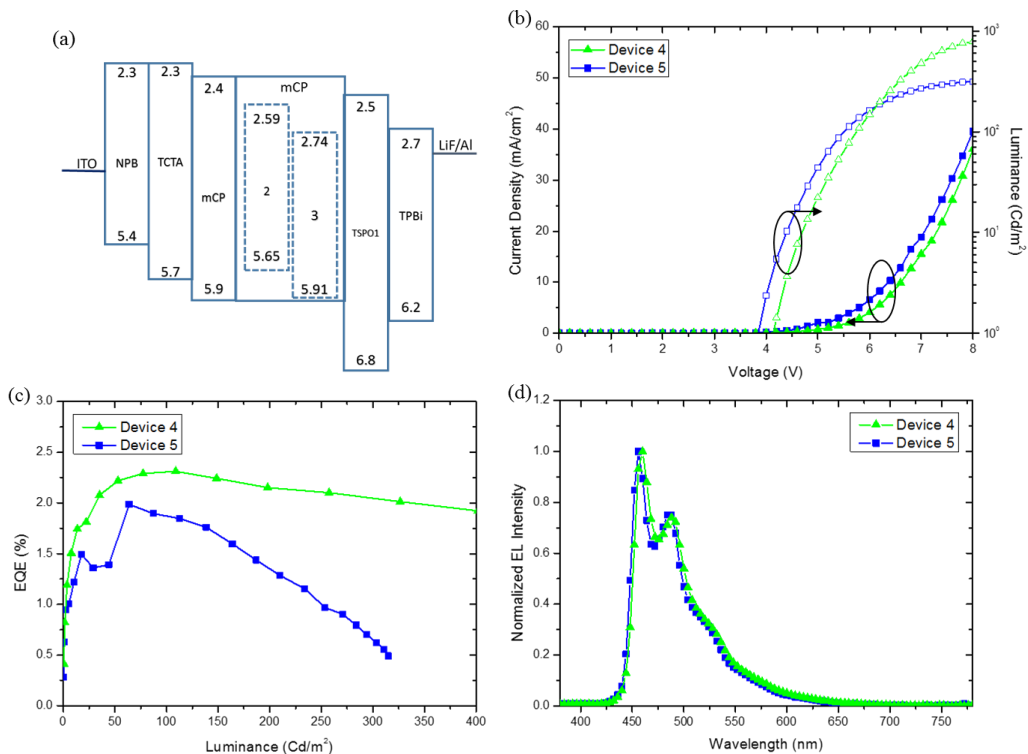
### Electroluminescent Properties

To evaluate the electroluminescent characteristics, organic light emitting devices were fabricated and optimized for efficient OLEDs was proceeded. Devices **1**, **2**, and **3** with simple structure OLEDs were fabricated using complexes **1**, **2**, and **3** as dopants, respectively. The structure of blue phosphorescent devices were as follows: ITO/TAPC (40 nm)/mCP: complexes **1-3** (8 wt%)(30 nm)/TPBi (40 nm)/LiF (1 nm)/Al (100 nm). TAPC and TPBi were used as hole and electron transporting layers, respectively. mCP was selected as a host materials because its HOMO and LUMO levels are well matched with those of complexes **1-3**.



**Figure 8.** (a) Device configuration and energy level diagram (b) J-V-L characteristics (c) External quantum efficiency versus luminescence (d) EL spectra of device **1-3**.

The device performances were shown in Figure 8 and summarized in Table 2. Device **2** using complex **2** as a dopant exhibited better performance than devices **1** and **3**, because higher current density in device **2**. As shown in Figure 8(b), the large HOMO energy gap between TAPC and mCP (0.4 eV) caused high turn-on voltage around 5 V. In Figure 8(d), additional peaks from TPBi are shown in the EL spectra. To solve these problems, devices **4** and **5** using complexes **2** and **3** were fabricated. The device structure is as follows: ITO/NPB (40 nm)/ TCTA (15 nm)/mCP (5 nm)/mCP: complexes **2** and **3** (8 wt%)(30 nm)/TSPO1 (5 nm)/TPBi (15 nm)/LiF (1 nm)/Al (100 nm). NPB and TCTA were

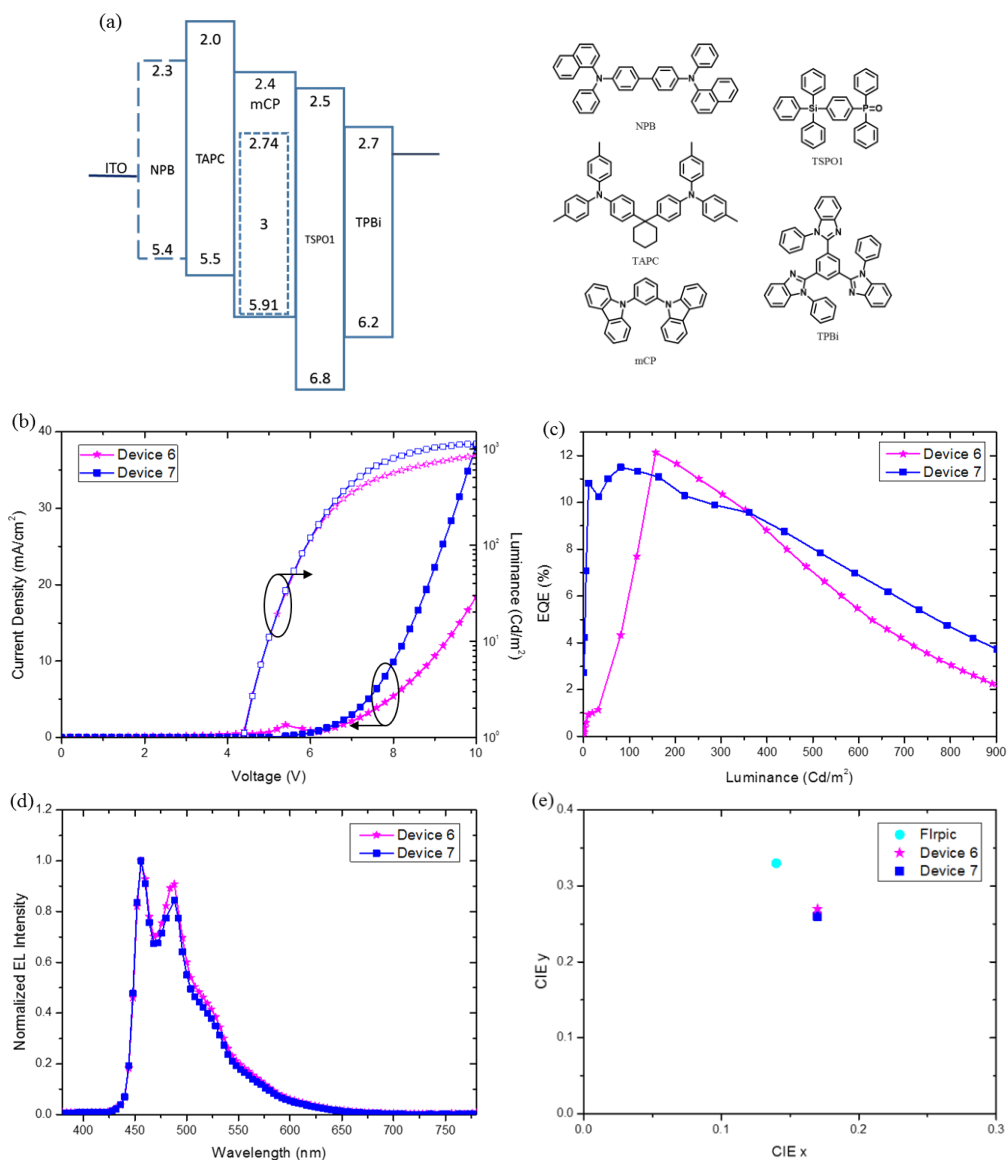


**Figure 9.** (a) Device configuration and energy level diagram (b) J-V-L characteristics (c) External quantum efficiency versus luminescence (d) EL spectra of device **4** and **5**.

selected as hole injecting and transporting layers to alleviate the hole injection barrier and lower turn-on voltage of the devices. Thin layers of mCP ( $E_T = 2.9$  eV) and TSPO1 ( $E_T = 3.36$  eV) were inserted as electron and hole blocking layers, respectively, to confine the triplet excitons in the emitting layer and induce emission only from emitters. The EL performances of devices **4** and **5** were illustrated in Figure 9 and summarized in Table 2. The turn-on voltages were lowered to 4 and 3.6 V for devices **4** and **5**. As shown in Figure 9(d), emission peaks from TPBi disappeared and the maximum emission peaks at 460 and 456 nm for devices **4** and **5**, respectively. However, devices **4** and **5** showed



inferior device performances compared to devices **2** and **3**. The complex device structure led current injection difficult and resulted in lower current efficiency and external quantum efficiency. Device **6** using complex **3** as an emitter was fabricated with a simple device structure: ITO/TAPC (40 nm)/mCP: complex **3** (8 wt%)(30 nm)/ TSPO1 (5 nm)/TPBi (45 nm)/LiF (1 nm)/Al (100 nm). We selected complex **3** as a dopant material for OLEDs, because complex **3** exhibited the deepest blue emission with moderate quantum efficiency. TAPC was used as hole injecting and transporting layer instead of NPB and TCTA and electron blocking layer was eliminated due to high triplet energy of TAPC ( $E_T = 2.9$  eV). As shown in Figure 10(c), device **6** exhibited outstanding performances with maximum external quantum efficiency of 12.1% at 6.2 V, but it showed a drastic decline in external quantum efficiency. A buffer layer used to smoothen the rough surface of ITO and prevent TAPC from crystallization was needed. Thus, NPB was inserted between the ITO and TAPC layer in device **7**, which has a structure as follows: ITO/NPB (20 nm)/TAPC (20 nm)/mCP: complex **3** (8 wt%)(30 nm)/TSPO1 (5 nm)/TPBi (45 nm)/LiF (1 nm)/Al (100 nm). The turn-on voltage was slightly increased to 4.4 V. At the practical brightness of 100 cd/m<sup>2</sup>, the driving voltage is 5.9 V while external quantum efficiency is 11.1 %. The maximum external quantum efficiency is 11.5%, as shown in Figure 10(c). Electroluminescent spectra are illustrated in Figure 10(d). The maximum emission appeared at 456 nm and no additional emissions from host or



**Figure 10.** (a) Device configuration, energy level diagram and molecular structures of organic layers (b) J-V-L characteristics (c) External quantum efficiency versus luminescence (d) EL spectra of device 6 and 7 (e) CIE coordinates of Flrpic and complex 3 based devices.

intimate layers were detected, illustrating high recombination efficiency between holes and electrons in the emitting layer. The emission profiles were mostly unchanged as driving voltage increases. This settled

emission according to the driving voltage can stably operate the device. The color coordinates were (0.17, 0.26) at 100 cd/m<sup>2</sup>. In Figure 10(e), color coordinates of devices **6** and **7** were compared with blue reference materials, FIrpic.<sup>10</sup> Without fluorine substitutes, complex **3** exhibited a lower color coordinate y value, which was comparable with commercially available blue phosphorescent emitters. Due to absence of fluorine moiety, we expect that devices using these three complexes will have better long term stability than devices with FIrpic.

**Table 2.** Electroluminescent properties of device **1-7**.

Device	Voltage (V)		Current Efficiency (Cd/A)		Power Efficiency (lm/W)		EQE (%)		EL <sub>max</sub> (nm)	CIE x,y
	turn-on	@ 100 cd/m <sup>2</sup>	@ 100 cd/m <sup>2</sup>	Max	@ 100 cd/m <sup>2</sup>	Max	@ 100 cd/m <sup>2</sup>	Max	@ 100 cd/m <sup>2</sup>	@ 100 cd/m <sup>2</sup>
<b>1</b>	5.0	15.0	5.20	8.08	2.16	2.67	3.24	4.96	460	(0.16, 0.26)
<b>2</b>	4.8	12.9	8.64	9.80	3.90	3.98	4.93	5.57	460	(0.18, 0.29)
<b>3</b>	5.0	13.8	8.14	8.72	3.38	3.80	4.64	4.78	456	(0.18, 0.28)
<b>4</b>	4.0	5.76	3.76	3.78	2.06	2.11	2.30	2.31	460	(0.17, 0.26)
<b>5</b>	3.8	5.52	2.91	3.09	1.67	1.87	1.87	1.99	456	(0.16, 0.24)
<b>6</b>	4.2	5.92	10.20	20.70	5.35	10.49	6.05	12.1	456	(0.17, 0.27)
<b>7</b>	4.4	5.92	18.65	19.17	9.95	10.38	11.1	11.5	456	(0.17, 0.26)

## Conclusions

In summary, we designed and synthesized fluorine-free blue phosphorescent iridium complexes. Three compounds exhibited 8-15 nm blue shifted emission compared to FIrpic with compatible quantum efficiency. This phenomena arises from replacing the pyridine ring with pyrimidine ring in cyclometalated ligands. With a proper selection of ancillary ligands, complexes **2** and **3** showed emissions at shorter wavelengths. The electroluminescent devices were fabricated successfully. In particular, the device **7** using complex **3** as an emitter, displayed EL maximum at 456 nm and gave maximum external quantum efficiency of 11.5 % at 5.9 V and a CIE coordinate of (x,y) = (0.17, 0.26) at a brightness of 100 cd/m<sup>2</sup>. The color coordinate is comparable to other well-known blue emitting materials with fluorine moieties. By further optimizing the device structure, better device performance can be attained with the fluorine-free heteroleptic iridium complexes.

## B.1.3. Experimental Sections

### Materials and methods

All reactions were performed under N<sub>2</sub> condition and solvent were distilled from appropriate drying agents before use. Commercially available reagents were purchased from Aldrich and Alfa and used without further purification. <sup>1</sup>H and <sup>13</sup>C NMR spectra were recorded with Bruker Avance DPX-300 in CDCl<sub>3</sub>. UV-vis absorption spectra were measured by Beckman Coulter DU-650 at room temperature. Emission spectra were recorded on Jasco FP-6500 at room temperature in dichloromethane (DCM). Quantum yield measurements were carried out at room temperature in degassed dichloromethane solution using Flrpic as a reference. Low temperature phosphorescence spectra were obtained by Jasco FP-6500 in 2-methyltetrahydrofuran at liquid nitrogen condition. Time resolved phosphorescence lifetime measurements were performed by the time correlated single photon counting (TCSPC) technique with a FluoTime200 spectrometer (PicoQuant) equipped with a NanoHarp 300 TCSPC board (PicoQuant) and a PMA182 photomultiplier (PicoQuant). The excitation source was a 342 nm picosecond pulsed diode laser (PicoQuant, PLS340) driven by a PDL800-D driver (PicoQuant). Mass spectra were measured by JMS-600W operating in fast atom bombardment (FAB) mode. Cyclic voltammetry was performed with CHI650B. The measurement used three electrode electrochemical cell in

0.1 M tetrabutylammonium perchlorate solution in dichloromethane with scan rate  $0.1 \text{ V s}^{-1}$  at room temperature. A glassy carbon, platinum wire and Ag/AgCl were used as working electrode, counter electrode and reference electrode, respectively. Ferrocene was used as internal standard.

## Synthesis

**Synthesis of ligands.** 2-tertbutylpyrimidine<sup>11</sup>, 5-bromo-2-tertbutyl pyrimidine<sup>12</sup>, 2-tert-butyl-5-(pyridin-2-yl)pyrimidine<sup>13</sup> were synthesized via reported procedures. Ancillary ligands were also produced by brief steps<sup>14</sup>.

**General Synthesis of Iridium Complexes.** A mixture of  $\text{IrCl}_3 \cdot n\text{H}_2\text{O}$  (0.19 g, 0.55 mmol, 0.5 equiv.) and b5ppmH (0.23 g, 1.1 mmol, 1 equiv.) in 2-methoxyethanol (40 mL) was refluxed for 24h. After cooling to RT, 2-picolinic acid (0.17 g, 1.4 mmol, 1.2 equiv.) and sodium carbonate (0.6 g, 5.5 mmol, 5 equiv.) were added. The mixture was then refluxed for 4h. The solvent was removed in vacuo. The residue was suspended with water then extracted with ethyl acetate twice. Combined organic layer was dried over sodium sulfate, evaporated under reduced pressure. The crude product was chromatographed using DCM-Methanol as an eluent.

*(b5ppm)<sub>2</sub>Ir(pic)* (**1**). Yellow solid, yield: 23%. <sup>1</sup>H NMR (300MHz,  $\text{CDCl}_3$ )  $\delta$  8.87 (d,  $J=5.7 \text{ Hz}$ , 1H), 8.45-8.39 (m, 3H), 8.00 (t,  $J=7.7 \text{ Hz}$ ,

1H), 8.02-7.78 (m, 5H), 7.64 (d,  $J=2.8$  Hz, 1H), 7.48 (t,  $J=6.9$  Hz, 1H), 7.27 (t,  $J=5.7$  Hz, 1H), 7.08 (t,  $J=6.3$  Hz, 1H), 1.14 (s, 9H), 1.05 (s, 9H).  $^{13}\text{C}$  NMR (300MHz,  $\text{CDCl}_3$ ) 180.5, 179.1, 175.4, 174.8, 172.4, 164.4, 163.1, 151.8, 150.2, 149.0, 148.3, 146.8, 146.7, 138.4, 137.7, 137.5, 136.9, 136.7, 128.4, 128.3, 122.8, 122.6, 118.4, 117.9, 39.1, 38.9, 29.5, 29.4. HRMS (FAB) calc'd  $[\text{M}+\text{H}]^+=740.2319$ , observed = 740.2327.

(*b5ppm*)<sub>2</sub>Ir(*mptz*) (**2**). Yellow solid, yield: 18%.  $^1\text{H}$  NMR (300MHz,  $\text{CDCl}_3$ )  $\delta$  8.46 (d,  $J=10.5$  Hz, 2H), 8.24 (d,  $J=7.9$  Hz, 1H), 7.96 (d,  $J=5.6$  Hz, 1H), 7.87 (dt,  $J=9.0, 1.2$  Hz, 1H), 7.82-7.71 (m, 5H), 7.65 (d,  $J=5.6$  Hz, 1H), 7.15 (t,  $J=6.0$  Hz, 1H), 7.10 (dt,  $J=5.8, 1.9$  Hz, 1H), 7.01 (t,  $J=5.9$  Hz, 1H), 2.51 (s, 3H), 1.12 (s, 9H), 1.07 (s, 9H).  $^{13}\text{C}$  NMR (300MHz,  $\text{CDCl}_3$ ) 186.5, 180.7, 175.6, 174.7, 164.1, 163.8, 163.5, 162.5, 152.0, 151.6, 149.4, 149.3, 147.0, 146.7, 138.7, 137.4, 137.3, 137.0, 136.1, 124.0, 123.1, 122.5, 121.1, 118.4, 118.0, 39.1, 38.9, 29.5, 14.6. HRMS (FAB) calc'd  $[\text{M}+\text{H}]^+=777.2748$ , observed = 777.2755.

(*b5ppm*)<sub>2</sub>Ir(*ptz*) (**3**). Yellow solid, yield: 18%.  $^1\text{H}$  NMR (300MHz,  $\text{CDCl}_3$ )  $\delta$  8.53-8.48 (m, 3H), 8.02 (t,  $J=6.6$  Hz, 1H), 7.85-7.74 (m, 6H), 7.63 (d,  $J=5.6$  Hz, 1H), 7.35 (t,  $J=6.1$  Hz, 1H), 7.09-6.98 (m, 2H), 1.15 (s, 9H), 1.08 (s, 9H).  $^{13}\text{C}$  NMR (300MHz,  $\text{CDCl}_3$ ) 183.9, 178.5, 175.9, 175.1, 163.9, 163.8, 163.3, 151.3, 149.8, 149.5, 149.2, 147.2, 147.1, 139.3, 137.7, 137.6, 137.2, 136.2, 125.9, 123.3, 123.1, 122.7, 118.6, 118.3, 39.2, 39.0, 29.5, 29.4. HRMS (FAB) calc'd  $[\text{M}+\text{H}]^+=764.2544$ , observed = 764.2551.

## **Thermal Analysis**

The thermal properties of three iridium complexes were characterized by thermogravimetric (TG) measurements. Decomposition temperatures ( $T_d$ ) were observed Q-5000 IR, respectively. The TGA measurement were performed at  $10\text{ }^\circ\text{C min}^{-1}$  under a nitrogen atmosphere.

## **Computational Method**

All calculation were performed using the Gaussian 09 program package. The geometry optimization of the ground state by density functional theory (DFT) was carried out using B3LYP functional with 6-31G(d) basis sets, except for LanL2DZ basis sets for Ir atoms.

## **OLED Fabrication and Measurement**

Patterned indium-tin-oxide (ITO)-coated glass substrates with  $15\Omega$  per square sheet resistance were washed by distilled water and isopropyl alcohol with sonication, then dried in vacuum oven. UV treatment for 10 min was proceeded before vacuum deposition. Organic light emitting devices were fabricated through high vacuum ( $2 \times 10^{-6}$  Torr) thermal evaporation method. 4,4',4''-Tris(carbazol-9-yl)-triphenylamine (TCTA), N,N'-Bis(naphthalen-1-yl)-N,N'-bis(phenyl)benzidine(NPB),



4,4'-Cyclohexylidenebis[N,N-bis(4-methylphenyl)benzenamine](TAPC), 1,3-Bis(N-carbazolyl)benzene (mCP), Diphenyl-4-triphenylsilylphenylphosphine oxide (TSPO1), 2,2',2''-(1,3,5-Benzinetriyl)-tris(1-phenyl-1-H-benzimidazole) (TPBi) were purchased from commercial sources and used without further purification. The electroluminescent properties were evaluated by PR-650 SpectraScan SpectraColorimeter as a source meter. Current-voltage-luminescence characteristics were recorded with a programmable electrometer equipped with current and voltage sources (Keithley 2400).

## B.1.4. References

1. (a) Chi, Y.; Chou, P. T., *Chem. Soc. Rev.* **2010**, *39*, 638-655; (b) Lamansky, S.; Djurovich, P.; Murphy, D.; Abdel-Razzaq, F.; Lee, H. E.; Adachi, C.; Burrows, P. E.; Forrest, S. R.; Thompson, M. E., *J. Am. Chem. Soc.* **2001**, *123*, 4304-4312.
2. (a) Xiao, L. X.; Chen, Z. J.; Qu, B.; Luo, J. X.; Kong, S.; Gong, Q. H.; Kido, J. J., *Adv. Mater.* **2011**, *23*, 926-952; (b) Liang, B.; Jiang, C. Y.; Chen, Z.; Zhang, X. J.; Shi, H. H.; Cao, Y., *J. Mater. Chem.* **2006**, *16*, 1281-1286.
3. Chou, P. T.; Chi, Y.; Chung, M. W.; Lin, C. C., *Coord. Chem. Rev.* **2011**, *255*, 2653-2665.
4. Lee, S. J.; Park, K. M.; Yang, K.; Kang, Y., *Inorg. Chem.* **2009**, *48*, 1030-1037.
5. Duan, T.; Chang, T. K.; Chi, Y.; Wang, J. Y.; Chen, Z. N.; Hung, W. Y.; Chen, C. H.; Lee, G. H., *Dalton Trans.* **2015**, *44*, 14613-14624.
6. Chang, C. H.; Ho, C. L.; Chang, Y. S.; Lien, I. C.; Lin, C. H.; Yang, Y. W.; Liao, J. L.; Chi, Y., *J. Mater. Chem. C* **2013**, *1*, 2639-2647.
7. (a) Seifert, R.; de Moraes, I. R.; Scholz, S.; Gather, M. C.; Lussem, B.; Leo, K., *Org. Electron.* **2013**, *14*, 115-123; (b) Sivasubramaniam, V.; Brodkorb, F.; Hanning, S.; Loebel, H. P.; van Elsbergen, V.; Boerner, H.; Scherf, U.; Kreyenschmidt, M., *J. Fluorine Chem.* **2009**, *130*, 640-649.
8. Jung, N.; Lee, E.; Kim, J.; Park, H.; Park, K. M.; Kang, Y., *Bull. Korean Chem. Soc.* **2012**, *33*, 183-188.
9. Li, J.; Djurovich, P. I.; Alleyne, B. D.; Yousufuddin, M.; Ho, N. N.; Thomas, J. C.; Peters, J. C.; Bau, R.; Thompson, M. E., *Inorg. Chem.* **2005**, *44*, 1713-1727.
10. Bin, J. K.; Cho, N. S.; Hong, J. I., *Adv. Mater.* **2012**, *24*, 2911-2915.
11. Wang, T. S.; Cloudsdale, I. S., *Synth. Commun.* **1997**, *27*, 2521-2526.
12. Pews, R. G., *Heterocycles* **1990**, *31*, 109-114.
13. Chang, C. H.; Wu, Z. J.; Chiu, C. H.; Liang, Y. H.; Tsai, Y. S.; Liao, J. L.; Chi, Y.; Hsieh, H. Y.; Kuo, T. Y.; Lee, G. H.; Pan, H. A.; Chou, P. T.; Lin, J. S.; Tseng, M. R., *ACS Appl. Mater. Interfaces* **2013**, *5*, 7341-7351.
14. (a) Orselli, E.; Kottas, G. S.; Konradsson, A. E.; Coppo, P.; Frohlich, R.; de Cola, L.; van Dijken, A.; Buchel, M.; Borner, H., *Inorg. Chem.* **2007**, *46*, 11082-11093; (b) Mansoori, Y.; Atghia, S. V.; Sanaei, S. S.; Zamanloo, M. R.; Imanzadeh, G.; Eskandari, H., *Polym. Int.* **2012**, *61*, 1213-1220.

# 플루오린 치환기 없는 청색 이리듐 발광체를

## 이용한 유기 발광 다이오드 개발

유기 발광 다이오드는 자발광, 고휘도, 높은 명암비, 빠른 응답속도, 얇은 두께 등과 같이 디스플레이에 필요한 여러 장점을 가지고 있기 때문에 많은 연구가 진행되어 왔다. 그 중 이리듐 복합체를 발광체로 사용하는 연구가 관심을 받고 있다. 이리듐 복합체는 열적, 전기 화학적 안정성, 짧은 들뜬 상태 수명, 높은 양자 효율, 용이한 발광 파장 조절 특성을 보인다. 높은 효율의 적색, 녹색 발광을 보이는 이리듐 복합체에 관한 연구는 많이 되어있다. 하지만, 높은 삼중항 에너지 때문에 청색 발광 이리듐 복합체에 대한 연구는 아직까지 넘어야 할 과제이다.

이리듐 복합체의 발광 파장 조절은 이리듐에 배위하고 있는 리간드의 치환기나 구조의 변화를 통해 가능하다. HOMO 는 주로 이리듐의 d 오비탈과 주 리간드 페닐 고리의  $\pi$  오비탈에 LUMO 는 주 리간드 피리딘 고리의  $\pi^*$  오비탈에 분포하는 것이 알려져 있다. 따라서 페닐 고리에 전자 끌개를 피리딘 고리에 전자 주개를 삽입하여 이리듐 복합체의 발광파장을 단파장 영역으로 이동시킬

수 있다. 청색 인광 발광체로 잘 알려진 FIrpic 은 페닐 고리에 플루오린을 삽입하여 단과장으로의 이동을 피하였다. 이와 같이 페닐 고리에 전자 끌개를 삽입하여 HOMO 를 안정화시켜 에너지 갭을 늘리는 방법이 많이 연구되었다. 하지만 전자 끌개로 주로 쓰이는 플루오린 계열의 치환기는 승화 정제나 소자 구동 시에 분해되는 문제를 야기한다. 따라서 본 연구에서는 플루오린을 배제한 청색 인광 발광체 개발에 관하여 논의하고자 한다.

큰  $\pi-\pi^*$  에너지 갭을 갖는 페닐피리미딘 주 리간드에 적절한 보조 리간드를 사용하여 455-463 nm에서 발광을 나타내는 것을 확인하였다. 가장 단과장에서 발광하는 3 번 복합체를 사용하여 유기 발광 다이오드를 제작하여 최대 11.5 %의 외부 양자 효율을 보였다. 또한 청색 발광체로 잘 알려진 FIrpic 에 필적할 만한 CIE 색좌표인 (0.17, 0.26)을 나타냈다. 플루오린 치환기가 없는 발광체를 사용하였기 때문에 긴 소자적 수명을 나타낼 것으로 예상된다. 추가적인 소자 제작을 통해 소자 특성 역시 개선될 여지가 있다.

**주요단어:** 청색, 플루오린 없는, 이리듐 복합체, 피리미딘, 유기 발광 다이오드

**학번:** 2014-22404